

# Semi-discrete quantum droplets and vortices

Xiliang Zhang<sup>1</sup>, Xiaoxi Xu<sup>1</sup>, Yiyin Zheng<sup>1</sup>, Zhaopin Chen<sup>2</sup>, Bin Liu<sup>1</sup>, Chunqing Huang<sup>1</sup>, Boris A. Malomed<sup>2,1</sup>, and Yongyao Li<sup>1,2\*</sup>

<sup>1</sup>*School of Physics and Optoelectronic Engineering, Foshan University, Foshan 528000, China*

<sup>2</sup>*Department of Physical Electronics, School of Electrical Engineering, Faculty of Engineering, and the Center for Light-Matter Interaction, Tel Aviv University, Tel Aviv 69978, Israel.*

We consider a binary bosonic condensate with weak mean-field (MF) repulsion, loaded in an array of nearly one-dimensional traps coupled by transverse hopping. With the MF force balanced by the effectively one-dimensional attraction, induced in each trap by the Lee-Hung-Yang correction (a result of quantum fluctuations around the MF state), stable semi-discrete quantum droplets (QDs) emerge in the array, as fundamental ones and vortex QDs, with winding numbers, at least, up to 5, in both tight-binding and quasi-continuous forms. The results provide the first realization of stable semi-discrete vortex solitons, including ones with multiple vorticity.

*Introduction and the model.* Recent works with binary Bose-Einstein condensates (BECs) have led to a breakthrough in studies of quantum matter, predicting and experimentally realizing ultradilute superfluids which spontaneously form quantum droplets (QDs). This possibility was predicted in the three-dimensional (3D) setting [1], as well as in its two- and one-dimensional (2D and 1D) reductions [2], on the basis of a system of coupled mean-field (MF) Gross-Pitaevskii equations (GPEs) with the Lee-Hung-Yang (LHY) corrections, that account for zero-point quantum fluctuations around MF states [3]. In 3D and 2D geometries, the LHY terms are repulsive, offering an option to stabilize the condensate against the collapse driven by the contact cross-attraction between the two components, which slightly exceeds self-repulsion in each component. This prediction, in turn, suggests a possibility to create stable multidimensional soliton-like states in the form of QDs, which is a problem of great interest for many branches of physics [4], a well-known challenging issue being stability of 2D and 3D solitons against the collapse. The prediction was quickly followed by the creation of quasi-2D [5, 6] and isotropic 3D [7, 8] QDs in a binary condensate of two different atomic states of <sup>39</sup>K atoms. The competition of long-range attractive interactions and LHY repulsion has also made it possible to create stable QDs in single-component condensates of dipolar atoms [9]–[13]. In addition to their significance to fundamental studies, QDs offer potential applications, such as the design of matter-wave interferometers [14].

An essential extension is the recent prediction of stable 3D [15] and 2D [16] two-component QDs with embedded vorticity and robust necklace-shaped clusters [17] (on the contrary, vortex QDs in single-component dipolar condensates were found to be unstable [18]). These predictions are significant too, as the stabilization of 2D and 3D vortex solitons is an especially challenging issue [4, 19].

The reduction of the two-component MF system with

the LHY corrections to the effectively 1D configuration (the binary condensate loaded in a cigar-shaped trap subject to strong transverse confinement [20–22]) drastically changes the setting, making the LHY term attractive, on the contrary to its repulsive sign in higher dimensions [2]. Accordingly, the most relevant case is one with the effective cubic MF repulsion (inter-component attraction being slightly weaker than the intrinsic repulsion in each component) competing with a quadratic term representing the LHY-induced attraction. Soliton-like states in this model were recently studied in detail, demonstrating Gaussian-like and flat-top shapes in the case of relatively small and large numbers of atoms, respectively [23]. The next natural step is the consideration of a tunnel-coupled pair of 1D waveguides, in which recent analysis has demonstrated spontaneous symmetry breaking of dual-core droplets [24] (similar systems, combining the LHY term and linear mixing between two components, was introduced in Refs. [25, 26]).

Further, the availability of optical lattices for experiments with BEC [27, 28] suggests one to consider a setting in the form of an array of 1D traps, each coupled by hopping to adjacent ones. Similar configurations were broadly considered in optics, in the form of parallel-coupled arrays of fibers and stacks of planar waveguides, in temporal- and spatial-domain forms, respectively [29]–[40]. In the combination with intra-core nonlinearity, these systems give rise to a class of 2D semi-discrete solitons, which are continuous objects along the guiding cores and discrete in the transverse direction [30, 31, 37, 40, 41].

In this work, we aim to introduce semi-discrete QDs in the system of transversely coupled nearly 1D matter-wave traps, filled by the binary condensate which features the combination of the weak MF repulsion and LHY-induced attraction in each trap. Subjects of special interest are semi-discrete solitary vortices, which were not considered previously. We produce stable solutions for both fundamental (zero-vorticity) and vortical semi-discrete QDs, with the winding number (alias the topological charge) up to  $S = 5$ . In the 2D continuum form, bright vortex solitons were produced in various models

---

\*Electronic address: yongyaoli@gmail.com

[42]–[57], [15, 16], the main issue being, as mentioned above, their stability. While the stabilization of vortex modes was theoretically elaborated in diverse forms, it was demonstrated experimentally only in strongly non-local media [60]. In settings with local nonlinearity, self-trapped solitary vortices were experimentally observed in quasi-stable transient forms [58, 59]. On the other hand, vortex solitons were predicted in 2D [61, 62] and 3D [63] fully discrete media, including stable 2D modes with  $S \geq 2$  [64]. Such quasi-discrete 2D states were created in photorefractive lattices [65, 66]. The robustness of semi-discrete vortex QDs produced by the analysis presented below, and available techniques for the work with QDs [5]–[8] suggest that the creation of novel topologically organized states in the form of semi-discrete vortex QDs is a relevant objective for experiments.

The setting outlined above is realized in the form of the system of linearly-coupled GPEs for the semi-discrete wave function,  $\psi_j(z, t)$  (in the basic case, it is the same for both components of the binary condensate), with longitudinal coordinate  $z$  and the transverse discrete one,  $j$ . The GPE system includes the cubic self-repulsion competing with the LHY-induced quadratic self-attraction. In a scaled form [2, 23], it is written as

$$i\partial_t \psi_j = -(1/2)\partial_{zz}\psi_j - (C/2)(\psi_{j+1} - 2\psi_j + \psi_{j-1}) + g|\psi_j|^2\psi_j - |\psi_j|\psi_j, \quad (1)$$

where  $C > 0$  is the rate of hopping between adjacent cores, the strength of the quadratic attraction is normalized to be 1, and  $g > 0$  is the strength of the cubic self-repulsion. It is relevant to mention the studies of fully discrete 1D and 2D solitons [67, 68], which are supported, similar to the present system, by the competition of self-attractive (cubic) and repulsive (quintic) onsite nonlinearities. Somewhat similar to results for the cubic-quintic nonlinearity, we here find many branches of zero-vorticity states, of onsite- and offsite-centered (alias bond-centered) types, which are chiefly stable, but tend to disappear with the increase of  $C$ , as the medium is approaching a quasi-continuum regime. However, in the present work we address semi-discrete modes (rather than fully discrete ones), and, which is most essential, include the consideration of semi-discrete vortices, with winding numbers  $1 \leq S \leq 5$ , that were not considered previously.

The total norm of the system, which is proportional to the number of atoms in the condensate,  $N = \sum_j \int_{-\infty}^{+\infty} |\psi_j(z)|^2 dz$ , is fixed by choosing its particular value. First, for states with vorticities  $S = 0$  and 1, the fixed value is  $N_{S=0,1} = 100$ , which is appropriate for plotting the results. For  $S \geq 2$ , it is convenient to fix larger values of  $N$ . With fixed  $N$ , two control parameters are  $C$  and  $g$ , that will be varied in the range of  $0 \leq C, g \leq 1$ . Although this range seems limited, it is sufficient for identifying all species of self-trapped states in the system and making conclusions about their stability. Along with the norm, the system conserves the total

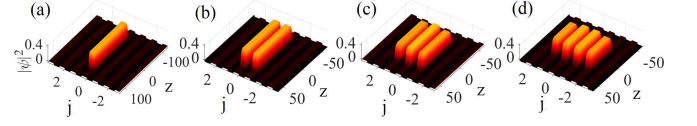


FIG. 1: Density profiles of coexisting stable onsite- and offsite-centered semi-discrete QDs with zero vorticity and the number of sites, in the discrete direction, from 1 to 4 in panels (a-d), respectively. Fixed parameters are  $(g, C, N) = (1, 0.01, 100)$ .

momentum along the continuous direction and energy,

$$E = \sum_j \int_{-\infty}^{+\infty} \left\{ \frac{1}{2} |(\psi_j)_z|^2 + C \left[ |\psi_j|^2 - \frac{1}{2} \psi_j^* (\psi_{j+1} + \psi_{j-1}) \right] + \frac{g}{2} |\psi_j|^4 - \frac{2}{3} |\psi_j|^3 \right\} dz \quad (2)$$

Stationary states with chemical potential  $\mu$  are looked for as  $\psi_j(z, t) = \phi_j(z)e^{-i\mu t}$ , where  $\phi_j(z)$  is a localized wave function. In the limit of  $C = 0$ , the uncoupled GPE (1) gives rise to 1D QDs. In particular, they assume the flat-top shape with a nearly constant density,  $|\phi|^2 = 4/(9g)$ , at  $\mu$  close to  $\mu_0 = 4/9 - 2/(3\sqrt{g})$ , at which the QD's width diverges [2, 23]. On the other hand, in the limit of  $g \rightarrow 0$  the QD takes a well-localized shape,  $\phi_{g=0}(z) = (3/2)|\mu_{g=0}|\text{sech}^2(\sqrt{|\mu_{g=0}|/2}z)$ , with  $\mu_{g=0} = -(1/3)(2N^2/3)^{1/3}$ .

The anisotropy of 2D QD in the  $(z, j)$  semi-discrete plane is defined as the ratio of its widths in the  $z$  and  $n$  directions,  $\varepsilon = \sqrt{C}L_z/L_j$ , with  $L_z \equiv \left[ \int_{-\infty}^{+\infty} |\phi_{j=0}(z)|^4 dz \right]^{-1} \left( \int_{-\infty}^{+\infty} |\phi_{j=0}(z)|^2 dz \right)^2$  and  $L_j \equiv \left[ \sum_j |\phi_j(z=0)|^4 \right]^{-1} \left[ \sum_j |\phi_j(z=0)|^2 \right]^2$ . Indeed, in the continuum limit, which corresponds to  $C \rightarrow \infty$ ,  $\varepsilon = 1$  implies that the 2D mode is axially symmetric in the plane of coordinates  $(z, j/\sqrt{C})$ . It is shown below that  $\varepsilon$  determines a boundary between tightly-bound and quasi-continuous ones semi-discrete states.

*Zero-vorticity QDs.* To generate stationary states, Eq. (1) was solved numerically by means of the imaginary-time-evolution method for finding QDs with zero vorticity  $S = 0$ , and squared-operator method [70] for constructing states with  $S \geq 1$ . Stability of the stationary states was then identified through computation of eigenvalues for small perturbations (not shown here in detail), and by dint of simulations of Eq. (1) in real time. Both approaches produce identical results, except for a specific case of slowly developing instability, shown below in Fig. 4(d), which may be a manifestation of a nonlinear instability, which is not indicated by unstable eigenvalues.

Two kinds of zero-vorticity modes, *viz.*, onsite- and offsite-centered ones, which occupy, respectively, odd and even numbers of sites,  $2J - 1$  and  $2J$ , in the discrete direction, are produced by the numerical solution. Starting

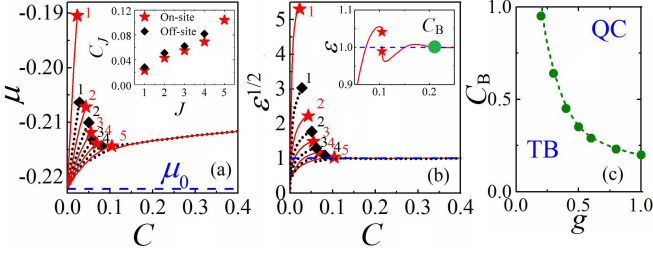


FIG. 2: (a,b) Dependences  $\mu(C)$  and  $\sqrt{\varepsilon(C)}$  for the onsite- and offsite-centered (red solid and black dotted lines, respectively) QDs with zero vorticity, built of  $2J-1$  or  $2J$  sites, versus  $J$ , at  $g = 1$ . The dashed line in (a) is  $\mu_0(g=1) \approx -0.222$ . These branches exist up to largest (terminal) values of  $J$ , viz.,  $J_T^{(\text{on})} = 5$  and  $J_T^{(\text{off})} = 4$ , respectively. The subplot in (a) shows critical values,  $C_J$ , at which the respective branches terminate, vs.  $J$ . The subplot in (b) displays the switch of the single eventually surviving onsite-centered mode from  $J = 5$  to  $J = 6$  with the subsequent increase of  $C$ . The green point, labeled  $C_B$ , at which  $\varepsilon$  attains value 1, is the boundary between the QDs with the tightly-binding (TB) and quasi-continuum (QC) structure, for  $g = 1$ . (c) The TB-QC boundary, designated by dependence  $C_B(g)$ .

from the anti-continuum limit,  $C \rightarrow 0$  [71], many coexisting solutions are found, corresponding to  $1 \leq J \leq 5$  and  $1 \leq J \leq 4$  for the onsite and offsite-centered types, respectively, i.e., with the number of sites from 1 to 9, see typical examples of stable semi-discrete modes with  $J = 1, 2$  in Fig. 1. The coexisting solution branches are represented by the respective dependences  $\mu(C)$  and  $\varepsilon(C)$ , for the above-mentioned fixed norm,  $N_{S=0,1} = 100$ , and a fixed value of  $g$ , in Figs. 2(a) and (b). The comparison of values of energy (2) for the modes found at the same values of  $(C, g, N)$  demonstrates that the energy minimum, i.e., the ground state, always corresponds to the largest number of sites.

The branches under the consideration originate from  $\mu = \mu_0$  and  $\varepsilon = 0$  at  $C = 0$ , and terminate at critical values  $C = C_J$  [69], which are denoted in Figs. 2(a) and (b) by red stars or black rhombuses for the odd and even states, respectively. The subplot in Fig. 2(a) shows  $C_J$  is a function of  $J$ , demonstrating that the multiplicity of coexisting branches reduces, step by step, with the increase of  $C$ . The single branch survives at  $C \geq 0.10$ , carrying over into the single nearly-isotropic fundamental mode with  $\varepsilon \rightarrow 1$  in the 2D quasi-continuous medium, as seen in Fig. 2(b). With the increase of  $C$ , the evolution of the single surviving state proceeds through the increase of the number of sites in this state. An elementary example is the transition from  $J = 5$  to  $J = 6$ , i.e., from 9 to 11 sites, with an incremental increase of  $C$ , as shown in the inset to Fig. 2(b).

The semi-discrete QDs can be categorized, roughly, as tightly-bound (TB) or quasi-continuous (QC) ones, if their shapes feature strong or weak discreteness, respectively. The consideration demonstrates that the bound-

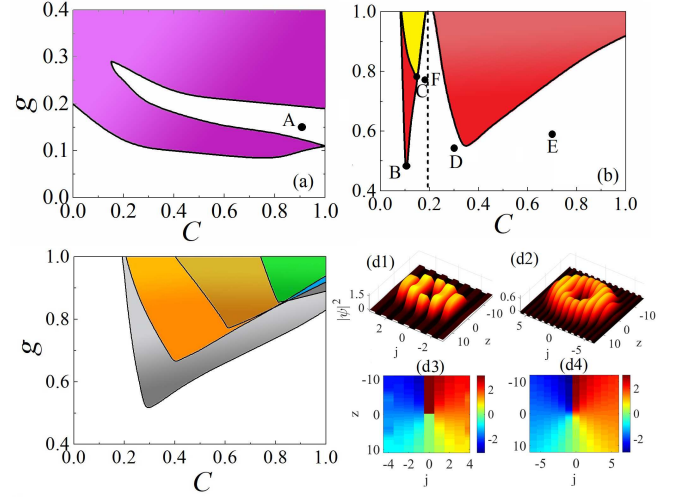


FIG. 3: (a) The stability area (purple) for offsite-centered semi-discrete QDs with zero vorticity, in the  $(C, g)$  parameter plane. Unstable modes, such as a typical one corresponding to point A, with  $(g, C) = (0.9, 0.15)$ , spontaneously transform into robust breathers, as shown in Fig. 4(a). Panel (b) displays stability areas for onsite- and intersite-centered vortex QDs with  $S = 1$  (yellow and red regions, and the yellow-only one, respectively). In panels (a) and (b), the fixed normalization is  $N = 100$ . (c) Stability areas for onsite-centered vortex modes with  $S = 2$  (all colored regions), 3 (orange + brown + green), 4 (brown + green + blue), and 5 (green + blue + dark gray). For the convenience of plotting, the normalization for  $S = 2$  through 5 is fixed as  $N = 400, 900, 2500$  and 4500, respectively. (d) Typical examples of stable onsite- and intersite-centered semi-discrete vortex QDs, for  $(g, C) = (0.48, 0.1)$  and  $(0.77, 0.15)$ , which correspond, severally, to points B and C in panel (c). Panels (d1,d2) and (d3,d4) display the respective density and phase profiles.

ary between these QD species is adequately determined by proximity of parameter  $\varepsilon$  to 1. A typical example of the transition from  $\varepsilon \neq 1$  to  $\varepsilon = 1$  is illustrated by the inset to Fig. 2(b), where  $C_B$  is identified as the transition point. A boundary between the TB and QC regimes in the  $(g, C)$  plane is displayed in Fig. 2(c). The decrease of the boundary value,  $C_B$ , with the increase of  $g$  is a natural trend, as stronger self-repulsion makes the droplet broader in the discrete direction, which is the same effect as produced by stronger inter-site hopping.

Analysis of the stability of the semi-discrete QDs with zero vorticity demonstrates that the onsite-centered modes are stable in the entire  $(g, C)$  plane, while their offsite-centered counterparts are stable only in a part of the plane, as shown in Fig. 3(a). The instability of the bond-centered states at small values of  $g$ , and their stabilization at larger  $g$ , is similar to findings for 1D discrete solitons in the model with the competing cubic-quintic nonlinearity [67]. However, a new feature, specific to the present system, is an inner lacuna in the stability area. In direct simulations, unstable offsite-centered QDs sponta-

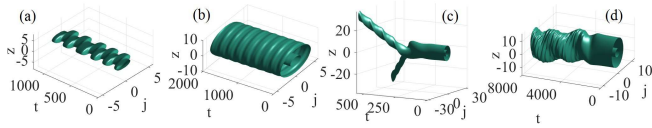


FIG. 4: (Color online) Examples of the evolution of unstable semi-discrete QDs. (a) The offsite-centered zero-vorticity QD denoted by point A in Fig. 3(a) transforms into a breather which performs shuttle motion. (b,c,d) Vortex QDs with  $(g, C) = (0.55, 0.3)$ ,  $(0.65, 0.6)$  and  $(0.75, 0.18)$ , which are denoted by points D-F in Fig. 3(d).

neously transform into robust breathers, which perform shuttle oscillations, as shown in Fig. 4(a).

*Vortex modes.* Semi-discrete states with intrinsic vorticity  $S$  represent a novel species of self-trapped modes, their stability being a central issue (especially for  $S > 1$ ), as suggested by studies of vortex solitons in various continuous models [19]. The present system gives rise to such states at  $g \geq g_{\min} \approx 0.4$ , which typically seem as quasi-isotropic modes, with  $\varepsilon$  close to 1. The systematic numerical analysis identifies stability areas for onsite-centered vortex QDs with  $S = 1$  and  $2 \leq S \leq 5$ , which are displayed in Figs. 3(b) and (c), respectively. For the vortices with  $S = 1$ , the stability area is split in two parts by a boundary of  $C \approx 0.19$  [the vertical dashed line in Fig. 3(b)], which is approximately equal to the boundary value,  $C_B$ , separating the TB and QC regions at  $g = 1$  in Fig. 2(d). Vortices with  $S \geq 2$  were found only at  $C > 0.19$ .

There are two different kinds of stable vortices with  $S = 1$ , onsite- and intersite-centered ones, with the pivot of the vortex located, respectively at a lattice site or between two sites. Stable intersite-centered vortices could be found only in a small (yellow) parameter region in Fig. 3(b) at  $C < 0.19$ , where the semi-discrete states feature a TB structure, and they do not exist with  $S \geq 2$ . These findings are natural, as in fully discrete 2D lattices it is also difficult to find stable intersite-centered vortex solitons, a relevant example being provided by the lattice with the cubic-quintic nonlinearity [68].

Figure 3(d1-d4) presents typical examples of stable onsite- and intersite-centered vortex QDs, which are taken near bottom edges of their stability area in the TB region [points B and C in Fig. 3(a)]. Because the value of  $g$  for the onsite-centered vortex in Fig. 3(d1) is relatively small,  $g = 0.48$ , it is strongly confined in the discrete coordinate, occupying only five sites.

In the QC region, i.e., at  $C > 0.19$ , stability areas for

onsite-centered semi-discrete vortices with  $2 \leq S \leq 5$  are displayed by means of different colors in Fig. 3(c), being similar to their counterpart with  $S = 1$  shown (also at  $C > 0.19$ ) in Fig. 3(b). In particular, the vortex QDs are stable at values of  $g$  exceeding a certain threshold, which gradually increases with the growth of  $S$ .

Unstable vortex QDs display different evolution scenarios. Close to the stability boundaries, they spontaneously develop into robust breathers which keep their initial winding numbers,  $S$ , see an example in Fig. 4(b). Another scenario occurs far away from the stability boundary. In this case, an unstable vortex QD spontaneously splits in two fragments, see an example in Fig. 4(c). A third type of the instability is observed, in Fig. 2(d), near the boundary between the TB and QC regions. In this case, unstable vortex modes undergo conspicuous deformation, but do not split, keeping their winding numbers and featuring an apparently chaotic evolution, see an example in Fig. 4d.

*Conclusion.* We have introduced a setting for the study of semi-discrete QDs in the form of the array of quasi-1D guides for matter waves coupled by hopping of atoms. Each guide is filled by a binary condensate, which gives rise to a semi-discrete system, in the form of the GPE including the LHY correction, i.e., repulsive cubic and attractive quadratic terms, and two coordinates, longitudinal continuous and transverse discrete ones. The systematic analysis has revealed many families of stable 2D semi-discrete QDs, of the onsite- and offsite-centered types, which terminate one by one with the increase of the transverse coupling coefficient. The system's parameter space is separated into TB (tight-binding) and QC (quasi-continuum) parts, with a single stable family surviving in the latter one. Previously unexplored self-trapped modes are semi-discrete vortices. In the TB region, vortex QDs, of both onsite- and intersite-centered types, exist and are stable with winding number  $S = 1$ , while in the QC region onsite-centered vortices have stability regions, at least, up to  $S = 5$ .

## Acknowledgments

This work was supported by NNSFC (China) through Grant No. 11874112, 11575063, Guangdong Provincial Department of Education Project through Grant No. 2018KQNCX279, and by the Israel Science Foundation through Grant No. 1286/17.

- 
- [1] D. S. Petrov, Quantum Mechanical Stabilization of a Collapsing Bose-Bose Mixture, *Phys. Rev. Lett.* **115**, 155302 (2015).
  - [2] D. S. Petrov and G. E. Astrakharchik, Ultradilute Low-Dimensional Liquids, *Phys. Rev. Lett.* **117**, 100401

(2016).

- [3] T. D. Lee, K. Huang, and C. N. Yang, Eigenvalues and Eigenfunctions of a Bose System of Hard Spheres and Its Low-Temperature Properties, *Phys. Rev.* **106**, 1135 (1957).

- [4] Y. Kartashov, G. Astrakharchik, B. Malomed, and L. Torner, *Frontiers in multidimensional self-trapping of nonlinear fields and matter*, *Nature Reviews Physics* **1**, 185-197 (2019).
- [5] C. R. Cabrera, L. Tanzi, J. Sanz, B. Naylor, P. Thomas, P. Cheiney, L. Tarruell, Quantum liquid droplets in a mixture of Bose-Einstein condensates, *Science* **359**, 301 (2018).
- [6] P. Cheiney, C. R. Cabrera, J. Sanz, B. Naylor, L. Tanzi, and L. Tarruell, Bright Soliton to Quantum Droplet Transition in a Mixture of Bose-Einstein Condensates, *Phys. Rev. Lett.* **120**, 135301 (2018).
- [7] G. Semeghini, G. Ferioli, L. Masi, C. Mazzinghi, L. Wolswijk, F. Minardi, M. Modugno, G. Modugno, M. Inguscio, and M. Fattori, Self-bound quantum droplets in atomic mixtures, *Phys. Rev. Lett.* **120**, 235301 (2018).
- [8] G. Ferioli, G. Semeghini, L. Masi, G. Giusti, G. Modugno, M. Inguscio, A. Gallemlé, A. Recati, and M. Fattori, Collisions of self-bound quantum droplets, *Phys. Rev. Lett.* **122**, 090401 (2019).
- [9] H. Kadau, M. Schmitt, M. Wenzel, C. Wink, T. Maier, I. Ferrier-Barbut, T. Pfau, Observing the Rosenzweig instability of a quantum ferrofluid, *Nature* **530**, 194-197 (2016).
- [10] I. Ferrier-Barbut, H. Kadau, M. Schmitt, M. Wenzel, T. Pfau, Observation of quantum droplets in a strongly dipolar Bose gas, *Phys. Rev. Lett.* **116**, 215301 (2016).
- [11] M. Schmitt, M. Wenzel, F. Böttcher, I. Ferrier-Barbut, and T. Pfau, Self-bound droplets of a dilute magnetic quantum liquid, *Nature*, **539**, 259 (2016).
- [12] L. Chomaz, S. Baier, D. Petter, M. J. Mark, F. Wächtler, L. Santos, and F. Ferlaino, Quantum-Fluctuation-Driven Crossover from a Dilute Bose-Einstein Condensate to a Macrodroplet in a Dipolar Quantum Fluid, *Phys. Rev. X* **6**, 041039 (2016).
- [13] H. Saito, Path-integral Monte-Carlo study on a droplet of a dipolar Bose-Einstein condensate stabilized by quantum fluctuation, *J. Phys. Soc. Jpn.* **85**, 053001 (2016).
- [14] B. Laburthe-Tolra, A strange kind of liquid, *Nature (London)* **539**, 176 (2016).
- [15] Y. V. Kartashov, B. A. Malomed, L. Tarruell, and L. Torner, Three-dimensional droplets of swirling superfluids, *Phys. Rev. A* **98**, 013612 (2018).
- [16] Y. Li, Z. Chen, Z. Luo, C. Huang, H. Tan, W. Pang, and B. A. Malomed, Two-dimensional vortex quantum droplets, *Phys. Rev. A* **98**, 063602 (2018).
- [17] Y. V. Kartashov, B. A. Malomed, and L. Torner, Metastability of quantum droplet clusters, *Phys. Rev. Lett.* **122**, 193902 (2019).
- [18] A. Cidrim, F. E. A. dos Santos, E. A. L. Henn, and T. Macrì, Vortices in self-bound dipolar droplets, *Phys. Rev. A* **98**, 023618 (2018).
- [19] B. A. Malomed, Vortex solitons: Old results and new perspectives, *Physica D*, in press; <https://doi.org/10.1016/j.physd.2019.04.009>.
- [20] M. Olshanii, V. Dunjko, and V. Lorent, Bosons in cigar-shaped traps: Thomas-Fermi, Tonks-Girardeau regime, and in between, *Phys. Rev. Lett.* **86**, 5413-5416 (2001).
- [21] L. Salasnich, A. Parola, and L. Reatto, Effective wave equations for the dynamics of cigar-shaped and disk-shaped Bose condensates, *Phys. Rev. A* **65**, 043614 (2002).
- [22] K. E. Strecker, G. B. Partridge, A. G. Truscott, and R. G. Hulet, Bright matter wave solitons in Bose-Einstein condensates, *New J. Phys.* **5**, 73 (2003).
- [23] G. E. Astrakharchik, and B. A. Malomed, Dynamics of one-dimensional quantum droplets, *Phys. Rev. A* **98**, 013631 (2018).
- [24] B. Liu, H. Zhang, R. Zhong, X. Zhang, X. Qin, C. Huang, Y. Li, B. A. Malomed, Symmetry breaking of quantum droplets in a dual-core trap, *arXiv:1901.06693*.
- [25] A. Cappellaro, T. Macrì, G. F. Bertacco, and L. Salasnich, Equation of state and self-bound droplet in Rabi-coupled Bose mixtures. *Sci. Rep.* **7**, 13358 (2017).
- [26] A. Tononi, Y. Wang, and L. Salasnich, Quantum solitons in spin-orbit-coupled Bose-Bose mixtures, *Phys. Rev. A* **99**, 063618 (2019).
- [27] M. Lewenstein, A. Sanpera, V. Ahufinger, B. Damski, A. Sen (De), and U. Sen, Ultracold atomic gases in optical lattices: Mimicking condensed matter physics and beyond, *Adv. Phys.* **56**, 243-379 (2007).
- [28] I. Bloch, J. Dalibard, and W. Zwerger, Many-body physics with ultracold gases, *Rev. Mod. Phys.* **80**, 885-964 (2008).
- [29] D. N. Christodoulides and R. I. Joseph, Discrete self-focusing in nonlinear arrays of coupled waveguides, *Opt. Lett.* **13**, 794-796 (1988).
- [30] A. B. Aceves, C. De Angelis, A. M. Rubenchik, and S. K. Turitsyn, Multidimensional solitons in fiber arrays, *Opt. Lett.* **19**, 329-331 (1994).
- [31] A. B. Aceves, G. G. Luther, C. De Angelis, A. M. Rubenchik, and S. K. Turitsyn, Energy localization in nonlinear fiber arrays: Collapse-effect compressor, *Phys. Rev. Lett.* **75**, 73-76 (1995).
- [32] Y. Liu, G. Bartal, D. A. Genov, and X. Zhang, Subwavelength discrete solitons in nonlinear metamaterials, *Phys. Rev. Lett.* **99**, 153901 (2007).
- [33] Y. V. Kartashov, V. A. Vysloukh, and L. Torner, Soliton shape and mobility control in optical lattices, *Prog. Opt.* **52**, 63-148 (2009).
- [34] F. Ye, D. Mihalache, B. Hu, and N. C. Panoiu, Subwavelength plasmonic lattice solitons in arrays of metallic nanowires, *Phys. Rev. Lett.* **104**, 106802 (2010).
- [35] A. Marini, A. V. Gorbach, and D. V. Skryabin, Coupled-mode approach to surface plasmon polaritons in nonlinear periodic structures, *Opt. Lett.* **35**, 3532-3534 (2010).
- [36] M. Conforti, C. De Angelis, and T. R. Akylas, Energy localization and transport in binary waveguide arrays, *Phys. Rev. A* **83**, 043822 (2011).
- [37] F. Eilenberger, S. Minardi, A. Szameit, U. Röpke, J. Kobelke, K. Schuster, H. Bartelt, S. Nolte, A. Tünnermann, and T. Pertsch, Light bullets in waveguide arrays: spacetime-coupling, spectral symmetry breaking and superluminal decay [Invited], *Opt. Exp.* **19**, 23711-23187 (2011).
- [38] T. Utikal, M. Hentschel, and H. Giessen, Nonlinear photonics with metallic nanostructures on top of dielectrics and waveguides, *Appl. Phys. B* **105**, 51-65 (2011).
- [39] Y. Kou, F. Ye, and X. Chen, Multipole plasmonic lattice solitons, *Phys. Rev. A* **84**, 033855 (2011).
- [40] R. Blit and B. A. Malomed, Propagation and collisions of semi-discrete solitons in arrayed and stacked waveguides, *Phys. Rev. A* **86**, 043841 (2012).
- [41] N. C. Panoiu, R. M. Osgood, and B. A. Malomed, Semi-discrete composite solitons in arrays of quadratically nonlinear waveguides, *Opt. Lett.* **31**, 1097-1099 (2006).
- [42] M. Quiroga-Teixeiro, H. Michinel, Stable azimuthal stationary state in quintic nonlinear optical media, *J. Opt.*



- Soc. Am. B **14**, 2004-2009 (1997).
- [43] I. Towers, A. V. Buryak, R. A. Sammut, and B. A. Malomed, Stable localized vortex solitons, *Phys. Rev. E* **63**, 055601(R) (2001).
  - [44] R. L. Pego and H. A. Warchall, Spectrally stable encapsulated vortices for nonlinear Schrödinger equations, *J. Nonlinear Sci.* **12**, 347-394 (2002).
  - [45] D. Mihalache, D. Mazilu, I. Towers, B. A. Malomed, and F. Lederer, Stable two-dimensional spinning solitons in a bimodal cubic-quintic model with four-wave mixing, *J. Optics A* **4**, 615-623 (2002).
  - [46] H. Saito and M. Ueda, Split instability of a vortex in an attractive Bose-Einstein condensate, *Phys. Rev. Lett.* **89**, 190402 (2002).
  - [47] B. B. Baizakov, B. A. Malomed, and M. Salerno, Multidimensional solitons in periodic potentials, *Europhys. Lett.* **63**, 642-648 (2003).
  - [48] J. Yang and Z. H. Musslimani, Fundamental and vortex solitons in a two-dimensional optical lattice, *Opt. Lett.* **28**, 2094-2096 (2003).
  - [49] S. K. Adhikari, Mean-field model of interaction between bright vortex solitons in Bose-Einstein condensates, *New J. Phys.* **5**, 137 (2003).
  - [50] D. Mihalache, D. Mazilu, F. Lederer, Y. V. Kartashov, L.-C. Crasovan, and L. Torner, Stable three-dimensional spatiotemporal solitons in a two-dimensional photonic lattice, *Phys. Rev. E* **70**, 055603(R) (2004).
  - [51] Y. V. Kartashov, V. A. Vysloukh, L. Torner, Stable ring-profile vortex solitons in Bessel optical lattices, *Phys. Rev. Lett.* **94**, 043902 (2005).
  - [52] D. Briedis, D. E. Petersen, D. Edmundson, W. Królikowski, and O. Bang, Ring vortex solitons in nonlocal nonlinear media, *Opt. Express* **13**, 435-443 (2005).
  - [53] A. I. Yakimenko, Y. A. Zaliznyak, and Y. Kivshar, Stable vortex solitons in nonlocal self-focusing nonlinear media, *Phys. Rev. E* **71**, 065603(R) (2005).
  - [54] Y. V. Kartashov, B. A. Malomed, Y. Shnir, and L. Torner, Twisted toroidal vortex solitons in inhomogeneous media with repulsive nonlinearity, *Phys. Rev. Lett.* **113**, 264101 (2014).
  - [55] H. Sakaguchi, E. Ya. Sherman, and B. A. Malomed, Vortex solitons in two-dimensional spin-orbit coupled Bose-Einstein condensates: Effects of the Rashba-Dresselhaus coupling and Zeeman splitting, *Phys. Rev. E* **94**, 032202 (2016).
  - [56] J. Qin, G. Dong, and B. A. Malomed, Stable giant vortex annuli in microwave-coupled atomic condensates, *Phys. Rev. A* **94**, 053611 (2016).
  - [57] S. Gautam and S. K. Adhikari, Vortex-bright solitons in a spin-orbit coupled spin-1 condensate, *Phys. Rev. A* **95**, 013608 (2017).
  - [58] F. Eilenberger, K. Prater, S. Minardi, R. Geiss, U. Röpke, J. Kobelke, K. Schuster, H. Bartelt, S. Nolte, A. Tünnermann, and T. Pertsch, Observation of discrete, vortex light bullets, *Phys. Rev. X* **3**, 041031 (2013).
  - [59] A. S. Reyna, G. Boudebs, B. A. Malomed, C. B. de Araújo, Robust self-trapping of vortex beams in a saturable optical medium, *Phys. Rev. A* **93**, 013840 (2016).
  - [60] Y. Izdebskaya, G. Assanto, and W. Królikowski, Observation of stable-vector vortex solitons, *Opt. Lett.* **40**, 4182-4185 (2015).
  - [61] B. A. Malomed and P. G. Kevrekidis, Discrete vortex solitons, *Phys. Rev. E* **64**, 026601 (2001).
  - [62] D. E. Pelinovsky, P. G. Kevrekidis, and D. J. Frantzeskakis, Persistence and stability of discrete vortices in nonlinear Schrödinger lattices, *Physica D* **212**, 20-53 (2005).
  - [63] P. G. Kevrekidis, B. A. Malomed, D. J. Frantzeskakis and R. Carretero-González, Three-dimensional solitary waves and vortices in a discrete nonlinear Schrödinger lattice, *Phys. Rev. Lett.* **93**, 080403 (2004).
  - [64] P. G. Kevrekidis, B. A. Malomed, Z. Chen, and D. J. Frantzeskakis, Stable higher-order vortices and quasivortices in the discrete nonlinear Schrödinger equation, *Phys. Rev. E* **70**, 056612 (2004).
  - [65] D. N. Neshev, T. J. Alexander, E. A. Ostrovskaya, Y. S. Kivshar, H. Martin, I. Makasyuk, and Z. G. Chen, Observation of discrete vortex solitons in optically induced photonic lattices, *Phys. Rev. Lett.* **92**, 123903 (2004).
  - [66] J. W. Fleischer, G. Bartal, O. Cohen, O. Manela, M. Segev, J. Hudock, and D. N. Christodoulides, Observation of vortex-ring “discrete” solitons in 2D photonic lattices, *Phys. Rev. Lett.* **92**, 123904 (2004).
  - [67] R. Carretero-Gonzalez, J. D. Talley, C. Chong, and B. A. Malomed, Multistable solitons in the cubic-quintic discrete nonlinear Schrödinger equation, *Physica D* **216**, 77-89 (2006).
  - [68] C. Chong, R. Carretero-González, B. A. Malomed, P. G. Kevrekidis, Multistable solitons in higher-dimensional cubic-quintic nonlinear Schrödinger lattices, *Physica D* **238**, 126-136 (2009).
  - [69] In fact, through saddle-node bifurcations generated by collision with additional branches of unstable solutions, which are not shown in the figure.
  - [70] J. Yang and T. I. Lakoba, Universally-convergent squared-operator iteration methods for solitary waves in general nonlinear wave equations, *Stud. Appl. Math* **118**, 153-197 (2007).
  - [71] J. L. Marin and S. Aubry, Breathers in nonlinear lattices: Numerical calculation from the anticontinuous limit, *Nonlinearity* **9**, 1501-1528 (1996).